ACS OMEGA

Article

Cite This: ACS Omega 2019, 4, 13100−13105

http://pubs.acs.org/journal/acsodf

# TOF-SIMS Analysis Using $Bi_3^+$ as Primary Ions on Au Nanoparticles Supported by $SiO_2$/Si: Providing Insight into Metal−Support Interactions

Il Hee Kim,[†,‡,∥] Byeong Jun Cha,[†,∥] Chang Min Choi,[‡] Jong Sung Jin,[§] Myoung Choul Choi,*[,‡] and Young Dok Kim*[,†]

[†]Department of Chemistry, Sungkyunkwan University, 2066, Seobu-ro, Suwon 16419, South Korea

[‡]Mass Spectrometry and Advanced Instrument Group, Korea Basic Science Institute, Ochang Center, 162, Yeongudanji-ro, Cheongju 28119, South Korea

[§]Division of High Technology Materials Research, Korea Basic Science Institute, Busan Center, 30, Gwahaksandan 1-ro 60beon-gil, Busan 46742, South Korea

Supporting Information

**ABSTRACT:** Au nanoparticles with a mean diameter of 20 nm with a coverage of ∼20% of the surface were distributed on a Si wafer surface and studied both before and after being annealed (at 100 and 300 °C). The two types of samples were analyzed using secondary ion mass spectroscopy (SIMS) with $Bi_3^+$ clusters as the primary ions combined with surface etching using $Ar_{1000}^+$ clusters. We observed a substantial difference in the SIMS spectra combined with a relatively short sputtering time of $Ar_{1000}^+$. In the nonannealed samples, bare Au cluster cations and $Si^+$ were observed in the SIMS spectra; $AuSi^+$ clusters were also observed in the annealed samples. These results indicate Au-silicide formation at a part of the periphery of the Au nanoparticles upon annealing. We suggest that SIMS experiments using cluster ions such as $Bi_3^+$ can not only be used for surface elemental analyses but also provide information on local chemical environments of elements on the surface. This is an important issue in heterogeneous catalysis (e.g., strong metal−support interactions). We also advise that one should be careful interpreting the SIMS data combined with a longer $Ar_{1000}^+$ sputtering time because this can deteriorate the surfaces from their original structures.

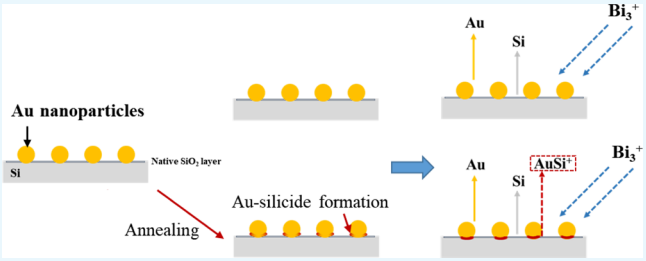


## 1. INTRODUCTION

In heterogeneous catalysis studies, surface analysis tools play a crucial role in unveiling the nature of active sites, such as their oxidation states and chemical environments, in catalytically active structures.[1−7] Most heterogeneous catalysts consist of catalytically active metal or metal oxide nanoparticles supported by high surface area oxides such as alumina and silica.[4,7−10] The nanoparticle−support interaction is very important because it not only determines stability of the nanoparticles but also the chemical nature of active sites at nanoparticle−support interfaces.[10−15]

Most surface analysis tools are based on the detection of low-energy electrons emitted from solid surfaces and are induced by either photons or high-energy electrons.[3−5,16−21] For example, X-ray and ultraviolet photoelectron spectroscopy (XPS) rely on photoemission processes,[3,5,16−18] whereas Auger electron spectroscopy and electron energy loss spectroscopy use high-energy electrons as primary particles.[4,10,19−21] These tools are useful for obtaining information about surface chemical compositions, electronic structures, and oxidation states of elements on solid surfaces. However, information about local coordination of atoms on surfaces, particularly heterogeneous surfaces such as oxides covered by metal or metal oxide nanoparticles, is not easy to obtain,[14,22−24] and it is difficult to determine whether atoms in nanoparticles and supporting materials interact chemically or physically at the interfaces. XPS can be used as a tool to obtain information about metal−support interactions. However, XPS peaks measured at the periphery and the core of the nanoparticles are often not easily separated, limiting its application in understanding metal−support interactions.[14,23,24]

In addition to these surface analysis methods, solid surfaces can be studied using mass spectrometry to measure secondary ions, which are emitted upon collision of accelerated primary ions, typically $Ar^+$, with the surface.[14,25−28] This method is referred to as secondary ion mass spectrometry (SIMS) and is useful for elemental analyses of solid surfaces. Dynamic SIMS, in which SIMS is combined with surface etching, provides the additional ability to conduct depth profile analyses.[26−28] This technique can be combined with other surface analysis

Received: April 6, 2019
Accepted: July 23, 2019
Published: August 5, 2019




DOI: 10.1021/acsomega.9b00985
ACS Omega 2019, 4, 13100−13105

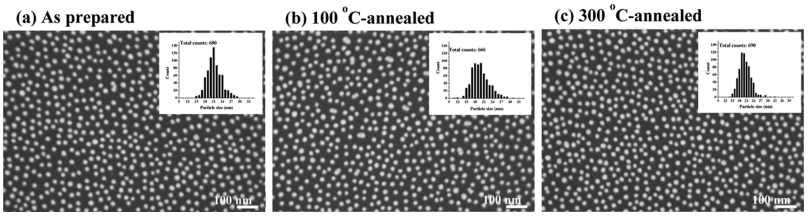


**Figure 1.** SEM images from (a) as-prepared Au/Si sample, (b) 100 °C-, and (c) 300 °C-annealed Au/Si samples, respectively. In each image, particle-size distribution is shown as inset.

techniques, such as XPS, and is particularly useful when surface impurities are removed before analysis under high-vacuum conditions.[29,30] Spectroscopic data obtained in combination with sputtering depth profile techniques should always be considered carefully because sputtering not only etches the surface layers but can also cause significant changes in the surface structure.[27,28] Therefore, interpretations of SIMS and depth-profile analyses are often limited to the qualitative elemental analyses; interpretations of the atoms' chemical environments are considered to be less reliable.

Previously, confirmation of Au-silicide formation during heat treatment and establishment of surface etching conditions to analyze the surface without varying the original structures were discussed.[26,34] In the present work, $Bi_3^+$ cluster cations were used as the primary ions of SIMS experiments for probing the chemical nature of Au nanoparticles supported by a Si wafer substrate. We anticipated that $Bi_3^+$ would etch the surface more softly than other ion sources (e.g., $Ga^+$, $Cs^+$, $Xe^+$, and $Ar^+$) due to its larger electron cloud size and polarizability. Therefore, $Bi_3^+$-SIMS is expected to provide more valuable information on the surface structure of the solid with much less deterioration during analysis compared to the other ion sources-based dynamic SIMS. We combined the $Bi_3^+$-SIMS with $Ar_{1000}^+$ sputtering to etch the surface of Au nanoparticles supported by a Si wafer. We determined that when $Bi_3^+$-SIMS is coupled with a relatively short $Ar_{1000}^+$ sputtering time, analyses of the secondary ions, both atomic species and clusters, can be useful for obtaining information on the local chemical environments of atoms on the surface. For example, emission of $AuSi^+$ as the secondary ion can be obtained only when Au and Si atoms chemically interact at part of the periphery of the Au nanoparticles. We highlight that cluster ion-based SIMS can be useful for obtaining valuable information on surface structures such as metal−support interaction in heterogeneous catalysis, which cannot be obtained using other surface analysis techniques.

## 2. RESULTS AND DISCUSSION

Figure 1 shows scanning electron microscopy (SEM) images of the Au nanoparticles distributed on Si wafer surfaces; the three images are from the original sample and the 100 and 300 °C post-annealed samples under atmospheric conditions. The Si surface is covered by native $SiO_2$ thin films. In each image, spherical Au nanoparticles with a mean diameter of ∼20 nm appear as bright spots, and the individual particles are separated from each other with a distance of several tens of nanometers. Structure and size of Au nanoparticles were also confirmed in transmission electron microscopy (TEM) image (Figure S2). The light and shade shown in the TEM image are likely due to polyhedral nature of the Au nanoparticles. SEM images show that neither of the annealing temperatures yielded significant changes in the shape or size of the Au particles.

In this study, a SIMS spectrum was obtained for each "cycle" of the experiment, where a cycle consists of $Ar_{1000}^+$ sputtering for 30 s with an acceleration voltage of 2.5 keV followed by collection of a SIMS spectrum using $Bi_3^+$ as the primary ions. Figure 2 shows a comprehensive SIMS spectrum, which was

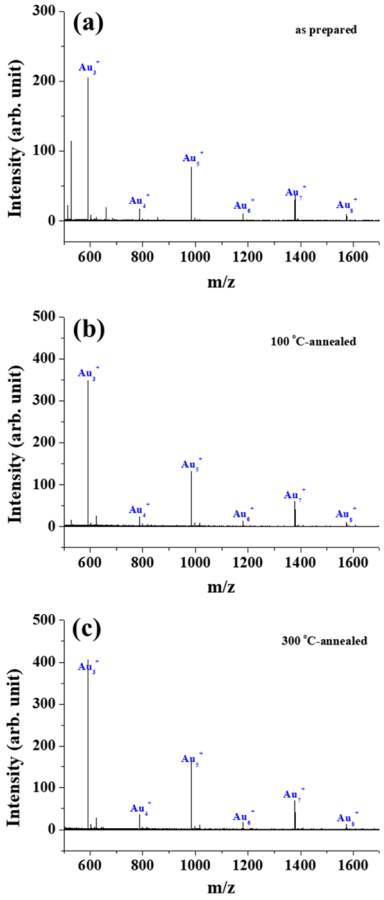


**Figure 2.** SIMS spectra collected from the surfaces of (a) as-prepared Au/Si sample, (b) 100 °C-, and (c) 300 °C-annealed Au/Si samples using $Bi_3^+$ as the primary ion are displayed in the $m/z$ range between 500 and 1700. See the text for more details about the procedure of collecting each spectrum.

achieved by accumulating individual SIMS spectra for the first 30 cycles. In the $m/z$ range above ∼550, one can observe multiple peaks separated by the same distance (noted in the Figure 2), corresponding to the mass of a single Au atom. The peaks in Figure 2 can be attributed to the Au cluster cations emitted by the collision of $Bi_3^+$ clusters with the Au/Si surface. Here, one can see the well-known, even-odd pattern, that is, the Au cluster cations with odd numbers of Au ions in a cluster are more abundant than even-numbered clusters.[26] Cluster



DOI: 10.1021/acsomega.9b00985
ACS Omega 2019, 4, 13100−13105

emission results from the collective excitation of Au atoms coordinated with each other within the same Au nanoparticle.[31,32] Cluster electronic structure can be explained by a one-electron shell model, where the valence electronic shells of a cluster are filled with the 6s Au atom electrons.[33] For odd-numbered cluster cations, there are an even number of valence electrons in a cluster, forming a closed electronic configuration that makes this cluster highly stable and abundant. On the other hand, the even-numbered cluster cations leave an unpaired electron in the outermost valence electronic shell of the cluster, yielding lower thermodynamic stability and abundance in the SIMS spectra. Not only the original samples, but also those post-annealed at 100 and 300 °C show this clear even-odd pattern from $Au_3^+$ to $Au_8^+$ with almost negligibly small amounts of $Au_mSi_n^+$. This implies that most of the Au atoms in a Au nanoparticle do not form alloys or chemically interact with the substrate's Si atoms, even after annealing.

In Figure 3, the mass spectra collected together with those in Figure 2 are displayed with the spectra in the lower $m/z$ range magnified. In contrast to the results shown in Figure 2, differences in the spectra are visible in Figure 3. The many peaks in the lower $m/z$ range are due to collisions of $Bi_3^+$ with the surface. This results not only in the emission of Au and Si, but also C, H, O, and N from organic ligands passivating the Au nanoparticles and impurities on the wafer surface. A closer inspection still shows that some peaks are derived from Au and Si. In the original sample, peaks corresponding to $Au^+$ and $Au_2^+$ can be identified (noted with arrows in Figure 3), with the intensity of $Au^+$ higher than that of $Au_2^+$ due to the even-odd cluster relationship explained previously. In contrast, the 100 °C-annealed samples reveal a new peak, which can be attributed to $AuSi^+$ cluster emission. This peak increases in intensity when the post-annealing temperature is increased to 300 °C. Some other peaks in Figure 3 were additionally assigned and are shown in Figure S4.

To better understand the emission behaviors of $Au^+$, $Au_3^+$, and $AuSi^+$ clusters, changes in the peak intensity as a function of cycles in our sputtering + SIMS experiments are shown in Figure 4. For comparison, the intensities of all of the species are normalized with respect to the total ion intensity of the SIMS spectrum in each depth analysis cycle. Changes of the respective $Si^+$ peaks are also shown for each sample. $Au_2^+$ was not plotted because its intensity was too low in all SIMS spectra. For the original sample, $Au^+$, $Au_3^+$, and $Si^+$ are visible, yet almost no $AuSi^+$ emission is seen for the first 20−30 cycles. Additional cycles resulted in the gradual increase of $AuSi^+$ peak

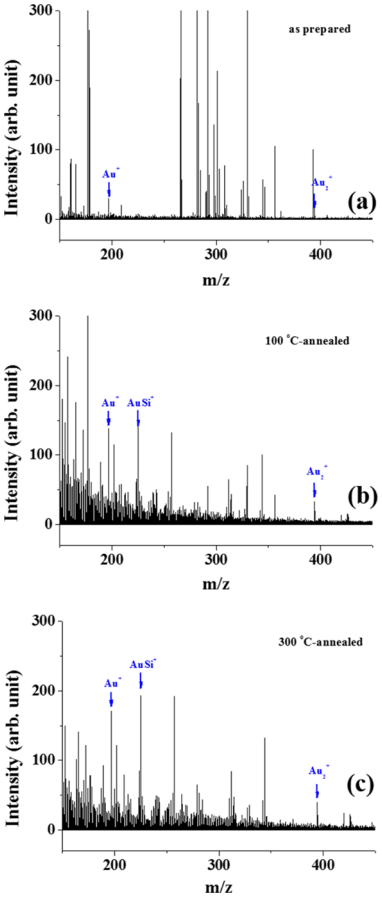


**Figure 3.** SIMS spectra collected from (a) as-prepared Au/Si sample, (b) 100 °C-, and (c) 300 °C-annealed Au/Si samples using $Bi_3^+$ as the primary ion are displayed in the $m/z$ range between 100 and 400. These spectra were collected together with those shown in Figure 2.

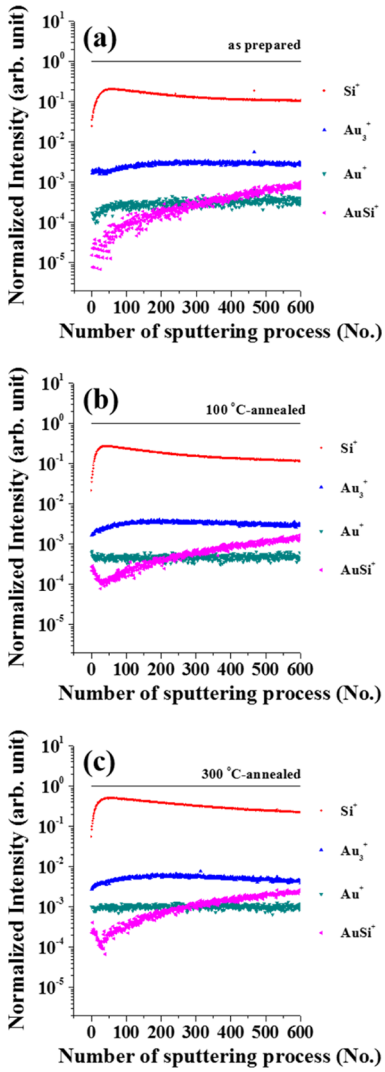


**Figure 4.** Change in the intensity of $Au^+$, $Au_2^+$, $Si^+$, and $AuSi^+$ signal as a function of number of sputtering + SIMS cycles collected from the surface of (a) as-prepared Au/Si sample, (b) 100 °C-, and (c) 300 °C-annealed Au/Si samples.



DOI: 10.1021/acsomega.9b00985
ACS Omega 2019, 4, 13100−13105

intensity. In contrast, for the post-annealed samples, $AuSi^+$, $Au^+$, and $Au_3^+$ are seen from the very beginning of our experiments, with less than 20 cycles of depth profile analysis.

In our previous studies, significant alloying of Au and Si resulted in the emission of $Au_mSi_n^+$ with both $m$ and $n$ values higher than 2 in the $Bi_3^+$ primary ion SIMS spectra.[26] In this study, such cluster cations were rarely seen in the SIMS spectra, implying that significant alloying of Au and Si did not occur, even after annealing. However, after annealing, $AuSi^+$ clusters could be found in the SIMS spectra from the early stage of the depth profile experiments; this species was barely seen in the original sample for the first 20−30 cycles of the experiment. Cluster emissions result from the collective excitation of coordinated atoms on the wafer surface by collision with primary ions. The $AuSi^+$ clusters can be emitted only when surface Au atoms are coordinated with neighboring Si atoms before the primary ion collision. Therefore, the results shown in Figures 3 and 4 indicate that there are almost no chemical interactions between Si and Au atoms in the original samples, but annealing induces formation of stronger chemical interactions between Au atoms with lower coordination numbers and neighboring Si atoms (Figure 5). XPS analysis

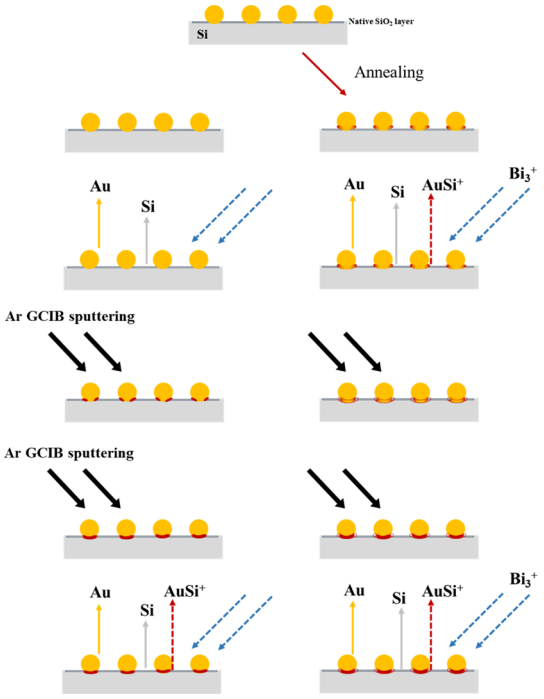


**Figure 5.** Schematic description of the structures of Au/Si samples, without and with post-annealing at 100 or 300 °C.

also evidenced formation of Au-silicide upon annealing but considering its weak intensity, Au-silicide could have been formed at only a part of the periphery of Au nanoparticles (Figure S5).

For better understanding of the formation of chemical bonds between Au and Si atoms during the annealing process, sputtering + SIMS experiments were conducted using Au/Si samples annealed at 50 and 75 °C (Figure S3a,b, respectively). At 50 °C, only a subtle change in the amount of $AuSi^+$ clusters was observed in comparison to the first 30 cycles for the original sample. However, when the annealing temperature was increased to 75 °C, an almost identical amount of $AuSi^+$ clusters were observed as those from the 100 °C- and 300 °C-annealed samples. A previous study revealed that Au-silicide could be formed at 25 °C.[34] In our samples, Au and Si alloys started to form at ∼ 50 °C, which is slightly warmer than room temperature, and at 75 °C, the Au and Si alloy formation at the periphery of the Au nanoparticles was almost complete.

It is not wholly understood why all of the samples, both with and without annealing, showed significantly large amounts of $AuSi^+$ emissions in the SIMS spectra when the number of cycles exceeded ∼100 (Figure 5). The original, non-annealed sample showed almost no $AuSi^+$ cluster emissions for the initial ∼20−30 cycles. However, $AuSi^+$ cluster emission from the original samples increased with increasing number of cycles, and for cycles greater than ∼200, the emission intensity of the original, non-annealed samples is very similar to the annealed samples in the SIMS spectra. This suggests that accumulated sputtering time along with an accelerated $Au_{1000}^+$ caused Au-silicide formation in the original samples. After 1100 cycles, the Au particle size and the texture of the Si wafer surface was very different from the original structure. In particular, the repeated sputtering + SIMS experiments resulted in an agglomeration of Au nanoparticles (Figure 6). This indicates that a large amount

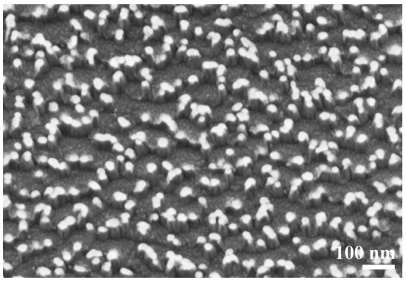


**Figure 6.** SEM image of the non-annealed Au/Si sample after 1100 cycles of $Ar_{1000}^+$-sputtering and subsequent $Bi_3^+$-SIMS experiment.

of energy was supplied to the surface during the experiments and was sufficient for inducing alloy formation from elements that originally interacted only weakly with their neighbors. Therefore, only SIMS data collected using very short accumulated sputtering times can be useful for unveiling the surface structures of solids. The $Au_{1000}^+$ clusters used for etching the surface are more easily polarized than $Ar^+$, which is widely used for dynamic SIMS experiments. Therefore, $Ar_{1000}^+$ clusters are expected to sputter the solid surface more softly when compared to $Ar^+$ ions with a similar acceleration voltage, although the SIMS data can only be combined with a very short sputtering time for surface structure analyses.

## 3. CONCLUSIONS

We synthesized Au nanoparticles with a mean diameter of ∼20 nm. The particles were distributed in the submonolayer of the surface of a Si wafer covered by native oxide layers. The original and post-annealed (100 and 300 °C) samples were analyzed using SIMS, with $Bi_3^+$ as the primary ions. These measurements were coupled with $Ar_{1000}^+$ sputtering to etch the surface layers. One experimental cycle consisted of Ar-cluster sputtering for 30 s followed by a SIMS experiment, allowing a SIMS spectrum to be obtained for each cycle. We studied the SIMS spectra of each sample as a function of the number of cycles. For the original, non-annealed sample, only $Au_n^+$ ($n$ = number of Au atoms) with a well-known even-odd pattern was observed during lower cycle frequency; no binary clusters of Au and Si were seen. In the annealed samples, $AuSi^+$ cluster



DOI: 10.1021/acsomega.9b00985
ACS Omega 2019, 4, 13100−13105

emissions were observed at similar cycle frequency. This result indicates that Au atoms form chemical bonds with Si at a part of the periphery of the Au nanoparticles upon annealing, and such subtle changes in the surface structure can be monitored using $Bi_3^+$-SIMS. Although few techniques (e.g., photoelectron emission microscopy and TEM) can give similar information, they are limited to well-defined surface structures, whereas $Bi_3^+$-SIMS can be applied even for much more complex surface structures with less crystallinity.[35,36] Using SIMS with cluster ions as the primary particles is a promising tool for obtaining information about the chemical environment of atoms on the surface of complex structures. We also showed that SIMS data obtained together with longer $Ar_{1000}^+$ sputtering times should be carefully interpreted because lengthy sputtering can induce structural changes to the solid surfaces.

## 4. EXPERIMENTAL SECTION

**4.1. Au Nanoparticle Synthesis.** Gold(III) chloride hydrate (20 mM, $HAuCl_4{\cdot}3H_2O$, ≥99.9%, Sigma-Aldrich) aqueous solution and trisodium citrate (38.8 mM, HOC-(COONa)($CH_2COONa)_2{\cdot}2H_2O$, Sigma-Aldrich) aqueous solution were used for the synthesis of Au nanoparticles. $HAuCl_4$ solution (20 mM, 5 mL) was mixed with 195 mL of distilled water (D.W.) in a 250 mL round bottom flask with reflux and heated. When the solution boiled vigorously, 10 mL of 38.8 mM of trisodium citrate solution was added. After the sodium citrate solution was added, the color of the $HAuCl_4$ solution changed from pale yellow to clear, transparent purple, dark purple, and finally, a red wine color. The solution continued to boil for additional 20 min to complete the reaction.

**4.2. Au Nanoparticle Deposition on the Si Wafer Substrate.** A p-doped Si(100) wafer was diced into 5 × 5 mm pieces and cleaned by sonication in piranha solution ($H_2SO_4$ 3 mL + $H_2O_2$ 1 mL) at 90 °C. After 30 min, the Si wafer pieces were cleaned with D.W. and ethanol and dried.

The surface of the clean Si wafer was functionalized with (3-aminopropyl)triethoxysilane (APTES, ≥98%, Sigma-Aldrich) by immersing in APTES solution (APTES 100 μL + anhydrous toluene 10 mL) for 60 min. Finally, the Si wafer was cleaned by sonication in toluene, washed with fresh toluene, dried, and annealed at 120 °C for 30 min using a furnace.

Au nanoparticles were deposited on the surface of the APTES-functionalized Si wafer by immersing the Si wafer in a Au nanoparticle solution for 90 min. Next, the Si wafer was washed with D.W. and dried. The Si wafers with Au nanoparticles (Au/Si) were annealed at 50, 75, 100, and 300 °C for 1 h under atmospheric conditions.

**4.3. Sample Characterization.** The Au-synthesized nanoparticles were analyzed using TEM (Tecnai $G^2$ Spirit TWIN, FEI Company). For TEM analysis, a droplet of the Au nanoparticle solution was dropped onto a carbon-coated copper grid (200 mesh, Electron Microscopy Science), and the surface was analyzed using SEM (S-4800, Hitachi). Before SEM analysis, the Au/Si sample was annealed at both 100 °C and 300 °C, and the sample surface structure images were compared with the original Au/Si sample. The surface of the original Au/Si sample was analyzed before and after the SIMS experiments as well.

**4.4. TOF-SIMS Studies.** Time-of-flight SIMS (TOF-SIMS) experiments were conducted using a TOF-SIMS 5 (ION-TOF GmbH, Münster, Germany). The instrument was equipped with an Ar gas cluster ion beam (GCIB) gun and a Bi liquid metal ion gun mounted orthogonally to each other and 45° to the sample surface (Figure S1). One cycle of the depth profile analysis was composed with Ar cluster ion sputtering and a subsequent SIMS analysis; an $Ar_{1000}^+$ cluster with an acceleration voltage of 2.5 keV and a beam current of 0.97 nA was used for sputtering, and $Bi_3^+$ primary ions with an acceleration voltage of 30 keV and a beam current of 0.31 pA was used for SIMS analysis. A 500 × 500 μm area of the sample was sputtered with Ar GCIB, but only the central 200 × 200 μm area of the sputtered area of the sample was analyzed with $Bi_3^+$ as the primary ion. Secondary ions were analyzed with TOF-mass spectroscopy (MS). The mass scale in the SIMS was calibrated using the mass of $H^+$, $CH_3^+$, $C_2H_5^+$, $C_3H_7^+$, and $C_4H_9^+$.

## ■ ASSOCIATED CONTENT

### Supporting Information

The Supporting Information is available free of charge on the ACS Publications website at DOI: 10.1021/acsomega.9b00985.

Experimental setup for TOF-SIMS; TEM image of Au/Si; result of Ar sputtering and SIMS experiment using Au/Si samples annealed at 50 and 75 °C; SIMS spectra of Au/Si samples with detailed peak assignment; and XP spectra of Au/Si samples with detailed analyzing conditions (PDF)

## ■ AUTHOR INFORMATION


### Corresponding Authors

*E-mail: cmc@kbsi.re.kr (M.C.C.).
*E-mail: ydkim91@skku.edu (Y.D.K.).

### ORCID

Chang Min Choi: 0000-0001-7708-9056
Young Dok Kim: 0000-0003-1138-5455

### Author Contributions

‖I.H.K. and B.J.C. contributed equally to this work.


### Notes

The authors declare no competing financial interest.

## ■ ACKNOWLEDGMENTS

This work was supported by the Basic Science Research Program through the National Research Foundation of Korea (NRF) funded by the Ministry of Education (2018R1D1A1B07040916), and a research grant from the Korea Basic Science Institute (D39613).

## ■ REFERENCES


(1) Ertl, G. Reactions at surfaces: From atoms to complexity (Nobel lecture). *Angew. Chem., Int. Ed.* **2008**, *47*, 3524−3535.

(2) Iablokov, V.; Barbosa, R.; Pollefeyt, G.; Van Driessche, I.; Chenakin, S.; Kruse, N. Catalytic CO oxidation over well-defined cobalt oxide nanoparticles: size-reactivity correlation. *ACS Catal.* **2015**, *5*, 5714−5718.

(3) Anderson, D. P.; Alvino, J. F.; Gentleman, A.; Qahtani, H. A.; Thomsen, L.; Polson, M. I. J.; Metha, G. F.; Golovko, V. B.; Andersson, G. G. Chemically-synthesised, atomically-precise gold clusters deposited and activated on titania. *Phys. Chem. Chem. Phys.* **2013**, *15*, 3917−3929.

(4) Girardon, J.; Quinet, E.; Gribovalconstant, A.; Chernavskii, P.; Gengembre, L.; Khodakov, A. Cobalt dispersion, reducibility, and surface sites in promoted silica-supported Fischer-Tropsch catalysts. *J. Catal.* **2007**, *248*, 143−157.




DOI: 10.1021/acsomega.9b00985
*ACS Omega* 2019, 4, 13100−13105

(5) Vass, E. M.; Hävecker, M.; Zafeiratos, S.; Teschner, D.; Knop-Gericke, A.; Schlögl, R. The role of carbon species in heterogeneous catalytic processes: an in situ soft x-ray photoelectron spectroscopy study. *J. Phys.: Condens. Matter* **2008**, *20*, 184016.
(6) Butcher, D. R.; Grass, M. E.; Zeng, Z.; Aksoy, F.; Bluhm, H.; Li, W.-X.; Mun, B. S.; Somorjai, G. A.; Liu, Z. In situ oxidation study of Pt(110) and its interaction with CO. *J. Am. Chem. Soc.* **2011**, *133*, 20319−20325.
(7) den Breejen, J. P.; Sietsma, J. R. A.; Friedrich, H.; Bitter, J. H.; de Jong, K. P. Design of supported cobalt catalysts with maximum activity for the Fischer-Tropsch synthesis. *J. Catal.* **2010**, *270*, 146−152.
(8) King, J. S.; Wittstock, A.; Biener, J.; Kucheyev, S. O.; Wang, Y. M.; Baumann, T. F.; Giri, S. K.; Hamza, A. V.; Baeumer, M.; Bent, S. F. Ultralow loading Pt nanocatalysts prepared by atomic layer deposition on carbon aerogels. *Nano Lett.* **2008**, *8*, 2405−2409.
(9) Joo, S. H.; Park, J. Y.; Tsung, C.-K.; Yamada, Y.; Yang, P.; Somorjai, G. A. Thermally stable Pt/mesoporous silica core-shell nanocatalysts for high-temperature reactions. *Nat. Mater.* **2009**, *8*, 126−131.
(10) Jacobs, G.; Ma, W.; Davis, B. H.; Cronauer, D. C.; Jeremy Kropf, A.; Marshall, C. L. Fischer-Tropsch Synthesis: TPR-XAFS Analysis of Co/Silica and Co/Alumina Catalysts Comparing a Novel NO Calcination Method with Conventional Air Calcination. *Catal. Lett.* **2010**, *140*, 106−115.
(11) Zhou, Y.; Peterson, E. W.; Zhou, J. Effect of nature of ceria supports on the growth and sintering behavior of Au nanoparticles. *Catal. Today* **2015**, *240*, 201−205.
(12) Zimmermann, S.; Urbassek, H. M. Sputtering of nanoparticles: Molecular dynamics study of Au impact on 20nm sized Au nanoparticles. *Int. J. Mass Spectrom.* **2008**, *272*, 91−97.
(13) Wan, H.-J.; Wu, B.-S.; Zhang, C.-H.; Xiang, H.-W.; Li, Y.-W.; Xu, B.-F.; Yi, F. Study on Fe-$Al_2O_3$ interaction over precipitated iron catalyst for Fischer-Tropsch synthesis. *Catal. Commun.* **2007**, *8*, 1538−1545.
(14) Grams, J.; Ura, A.; Kwapiński, W. ToF-SIMS as a versatile tool to study the surface properties of silica supported cobalt catalyst for Fischer-Tropsch synthesis. *Fuel* **2014**, *122*, 301−309.
(15) de la Peña O'Shea, V. A.; Homs, N.; Fierro, J. L. G.; Ramírez de la Piscina, P. Structural changes and activation treatment in a Co/$SiO_2$ catalyst for Fischer−Tropsch synthesis. *Catal. Today* **2006**, *114*, 422−427.
(16) Chusuei, C. C.; Brookshier, M. A.; Goodman, D. W. Correlation of relative X-ray photoelectron spectroscopy shake-up intensity with CuO particle size. *Langmuir* **1999**, *15*, 2806−2808.
(17) Ono, L. K.; Roldan Cuenya, B. Formation and thermal stability of $Au_2O_3$ on gold nanoparticles: size and support effects. *J. Phys. Chem. C* **2008**, *112*, 4676−4686.
(18) Mudiyanselage, K.; Senanayake, S. D.; Feria, L.; Kundu, S.; Baber, A. E.; Graciani, J.; Vidal, A. B.; Agnoli, S.; Evans, J.; Chang, R.; Axnanda, S.; Liu, Z.; Sanz, J. F.; Liu, P.; Rodriguez, J. A.; Stacchiola, D. J. Importance of the Metal-Oxide Interface in Catalysis: In Situ Studies of the Water-Gas Shift Reaction by Ambient-Pressure X-ray Photoelectron Spectroscopy. *Angew. Chem., Int. Ed.* **2013**, *52*, 5101−5105.
(19) Goodman, D.; Kelley, R. D.; Madey, T. E.; Yates, J. T. Kinetics of the hydrogenation of CO over a single crystal nickel catalyst. *J. Catal.* **1980**, *63*, 226−234.
(20) Yao, Y.; Goodman, D. W. New insights into structure-activity relationships for propane hydrogenolysis over Ni-Cu bimetallic catalysts. *RSC Adv.* **2015**, *5*, 43547−43551.
(21) Hong, J.; Chu, W.; Chernavskii, P. A.; Khodakov, A. Y. Cobalt species and cobalt-support interaction in glow discharge plasma-assisted Fischer-Tropsch catalysts. *J. Catal.* **2010**, *273*, 9−17.
(22) Ellis, P. J.; Fairlamb, I. J. S.; Hackett, S. F. J.; Wilson, K.; Lee, A. F. Evidence for the surface-catalyzed Suzuki-Miyaura reaction over palladium nanoparticles: An operando XAS study. *Angew. Chem., Int. Ed.* **2010**, *49*, 1820−1824.
(23) Radnik, J.; Mohr, C.; Claus, P. On the origin of binding energy shifts of core levels of supported gold nanoparticles and dependence of pretreatment and material synthesis. *Phys. Chem. Chem. Phys.* **2003**, *5*, 172−177.
(24) Peters, S.; Peredkov, S.; Neeb, M.; Eberhardt, W.; Al-Hada, M. Size-dependent XPS spectra of small supported Au-clusters. *Surf. Sci.* **2013**, *608*, 129−134.
(25) Jacek, G. Surface studies of heterogeneous catalysts by time-of-flight secondary ion mass spectrometry. *Eur. J. Mass Spectrom.* **2010**, *16*, 453−461.
(26) Park, E. J.; Choi, C. M.; Kim, I. H.; Kim, J.-H.; Lee, G.; Jin, J. S.; Ganteför, G.; Kim, Y. D.; Choi, M. C. Dynamic secondary ion mass spectroscopy of Au nanoparticles on Si wafer using $Bi_3^+$ as primary ion coupled with surface etching by Ar cluster ion beam: The effect of etching conditions on surface structure. *J. Appl. Phys.* **2018**, *123*, 015303.
(27) Sarkar, D. K.; Bera, S.; Dhara, S.; Nair, K. G. M.; Narasimhan, S. V.; Chowdhury, S. XPS studies on silicide formation in ion beam irradiated Au/Si system. *Appl. Surf. Sci.* **1997**, *120*, 159−164.
(28) Yang, L.; Seah, M. P.; Gilmore, I. S.; Morris, R. J. H.; Dowsett, M. G.; Boarino, L.; Sparnacci, K.; Laus, M. Depth profiling and melting of nanoparticles in secondary ion mass spectrometry (SIMS). *J. Phys. Chem. C* **2013**, *117*, 16042−16052.
(29) Simpson, R.; White, R. G.; Watts, J. F.; Baker, M. A. XPS investigation of monatomic and cluster argon ion sputtering of tantalum pentoxide. *Appl. Surf. Sci.* **2017**, *405*, 79−87.
(30) Sundaravel, B.; Sekar, K.; Kuri, G.; Satyam, P. V.; Dev, B. N.; Bera, S.; Narasimhan, S. V.; Chakraborty, P.; Caccavale, F. XPS and SIMS analysis of gold silicide grown on a bromine passivated Si(111) substrate. *Appl. Surf. Sci.* **1999**, *137*, 103−112.
(31) Wittmaack, K. On the mechanism of cluster emission in sputtering. *Phys. Lett.* **1979**, *69*, 322−325.
(32) Betz, G.; Husinsky, W. Modelling of cluster emission from metal surfaces under ion impact. *Philos. Trans. R. Soc. London, Ser. A* **2004**, *362*, 177−194.
(33) de Heer, W. A. The physics of simple metal clusters: Experimental aspects and simple models. *Rev. Mod. Phys.* **1993**, *65*, 611.
(34) Chang, J. F.; Young, T. F.; Yang, Y. L.; Ueng, H. Y.; Chang, T. C. Silicide formation of Au thin films on (100) Si during annealing. *Mater. Chem. Phys.* **2004**, *83*, 199−203.
(35) Ghatak, J.; Sundaravel, B.; Nair, K. G. M.; Satyam, P. V. Ion-beam-induced enhanced diffusion from gold thin films in silicon. *J. Phys.: Condens. Matter* **2008**, *20*, 485008.
(36) Batabyal, R.; Mahato, J. C.; Roy, A.; Roy, S.; Bischoff, L.; Dev, B. N. Lateral straggling and its influence on lateral diffusion in implantation with a focused ion beam. *Nucl. Instrum. Methods Phys. Res., Sect. B* **2011**, *269*, 856−860.



DOI: 10.1021/acsomega.9b00985
*ACS Omega* 2019, 4, 13100−13105